

Recent Advances in Biomedical Image Segmentation Using Neural Networks

Cecilia Irene Loeza Mejía¹, Balzhoyt Roldán Ortega¹, R.R. Biswal²,
Gregorio Fernández Lambert¹, D. Reyes González¹

¹ Tecnológico Nacional de México,
Departamento de Posgrado e Investigación,
Mexico

² Escuela de Ingeniería y Ciencias,
Tecnológico de Monterrey, Zapopan, Jalisco,
Mexico

rroshanb@tec.mx

Abstract. In recent years, the analysis and processing of biomedical images had considerable relevance, as it has proven to be an effective way of obtaining information regarding human body in a less invasive way and thus helps in extracting the characteristics that could potentially represent a disease. Different aspects of segmentation algorithms and features have been largely studied in the last decade relating to various areas. However, there is not a single method or solution because of the variation in the property of images, medical imaging techniques and modalities, variability and noise for each object of interest. This work presents a comparison of different methods including deep learning for segmentation of multimodal biomedical images. In addition, the application of U-Net architecture for the lung region segmentation of chest computed tomography in the Lung TIME dataset was evaluated.

Keywords: Segmentation, biomedical image, neural networks.

1 Introduction

Biomedical images are especially important and have contributed to the progress of medicine, allowing us to see the human body in a less invasive way, helping to provide an efficient diagnosis. The information regarding internal structures, molecular composition and interaction of human body is crucial to evaluate the changes that occur over time for personalized treatment.

There are different kinds of physical processes that allow biomedical images to be generated [1]. These processes are mainly based on (i) ultrasound backscattering (ii) X-ray transmission: radiography, computed tomography (CT), (iii) Gamma ray emission from radioisotopes: Positron emission tomography (PET) and (iv) Spin precession in

magnetic fields: magnetic resonance imaging (MRI). In addition, there are multiple imaging modalities which can be (i) two dimensional ($M \times M$ pixels) or (ii) three-dimensional ($M \times M \times M$ voxels).

Medical image processing allows the analysis of a large amount of information quickly and efficiently, with the aim of searching for certain characteristics and identifying a certain group of diagnoses. Segmentation is often the first stage in pattern recognition systems [2] and it is an exceedingly difficult problem in any image [3]. Segmentation is an important tool in medical image processing because it directly affects the accuracy and reliability of the diagnosis results [4].

Moreover, it is used for feature extraction, quantification of measurements, and allows an image to be transformed to a more meaningful form, as it obtains region of interest (ROI) with similar features in an orderly manner and groups them into a class [6]. ROI possesses a group of pixels defined in different forms such as circle, ellipse, polygon or irregular shapes [7]. Segmentation is used, for example: for the detection of organs and to distinguish pathological tissue from normal tissue [2, 8]. In this article, segmentation in the spinal cord, spine, prostate, breast, lung, arteries and brain was reviewed. In addition, U-Net has been implemented for segmentation of the pulmonary region.

This paper is organized as follows: in the second section a review of segmentation techniques based on neural networks in the multimodal biomedical imaging (obtained from computed tomography scan, magnetic resonance imaging, ultrasound or collecting images over time [6]) is presented. The third section shows the materials and methods that were used in segmentation of chest computed tomography. The fourth section shows the results obtained in the segmentation of the pulmonary region and the comparison with the results of different neural networks and tools for segmentation. While, the last section a summary of segmentation in medical image processing and areas of improvement in neural networks.

2 Background

2.1 Techniques before Segmentation

Data augmentation. It allows modifying samples of the dataset to create more training images, which reduces the possibility of over-fitting [11] and improves the generalization of machine learning models. Zhuang et al. [4] used shift (vertical and horizontal), shear transformation and flipping about the horizontal plane on the training dataset. In contrast, Almajalid et al. [5] used rotation ($\pm 90^\circ$ in each time) and elastic deformations [26].

Dabiri et al. [11] used random rotation, horizontal and vertical flip transformations. Instead Gros et al. [16] included shifting (± 10 voxels in each direction), flipping, rotation ($\pm 20^\circ$ in each direction), and elastic deformations [26]. In contrast Van et al. [25] applied random amounts of translation, rotation, scaling, shearing, elastic warping, cropping, blurring, contrast alterations, noise addition, and mirroring in the anterior-posterior axis.

Instead Li et al. [17] applied rotation, horizontal flipping, zoom, height/width shift. Moreover Rat et al. [18] extracted randomly displaced image patches up to 3 voxels along each dimension of the image domain.

Pre-processing. At this stage, generally, the image noise is eliminated, and the contrast is improved. In biomedical images, morphological filters can be applied. To preprocess computed tomography (CT) images, the authors use morphological image processing, region-based image processing, and contrast adjustment [9], instead Dabiri et al. [11] converted DICOM images to grayscale PNG images and standardized their pixel value lie in the range of [0,1]. On the other hand, to preprocess magnetic resonance imaging (MRI) Ilhan et al. [20] applied morphological operations and pixel subtraction operations, in contrast, Gros et al. [16] used CNN to detect and crop parts of the image. Moreover, Lu et al. used [31] classical z-score normalization algorithm, Sheela et al. [32] applied median filter. To preprocess Yang et al. [33] applied N4 bias field correction algorithm and intensity normalization. Instead, to preprocess ultrasound images, Almajalid et al. [5] used Speckle Reducing Anisotropic Diffusion and histogram equalization; in contrast Nithya et al. [21] used the median filter.

2.2 Segmentation

The segmentation of biological images typically consists of partitioning an image into multiple regions of interest representing anatomical objects, for an efficient analysis and visualization. The different technical challenges and difficulties that are encountered during image segmentation procedures include, but not limited to, heterogeneous pixel intensities, noisy boundaries, and non-regular shapes with high variability.

There are several approaches to segmentation using machine learning, which can be supervised and unsupervised. The segmentation techniques are region-based, edge-based and multispectral or multimodal, which is based on integration of information from several images.

In addition, there are hybrid approaches, which result from the combination of individual procedures [3]. The Table 1 shows the neural networks techniques used in multimodal biomedical images.

The type of technique used may varies according to the type of biomedical image. Vania et al. [9] used in CT CNN and FCN, instead Liu et al. [10] used CDP-ResNet, alternately Dabiri et al. [11] Liu et al. [27] and Huang et al. [28] used DNN, instead Lessman et al. [14] used FCN.

On the other hand in MRI images, Lessman et al. [14] used FCN, instead Bui et al. [15] implement 3D-SkipDenseSeg, instead Gros et al. [16] applied CNN, by contrast Li et al. [17] used MMAN, Rak et al. [18] implement a combination of CNN and graph cuts and Tong et al. [30] proposed RIANet.

Moreover, in ultrasound images, Zhuang et al. [4] implement RDAU-NET, Almajalid et al. [5] used U-Net, Karimi et al. [22] and Xu et al. [23] applied CNN, instead Yang et al. [29] DPU-Net.

Table 1. Segmentation strategies in Biomedical Images.

Abbreviation	Technique	Aspect of interest
CNN	Convolutional Neural Network	It requires a minimum preprocessing and extract features from image pixel [5].
CDP-ResNet	Cascaded Dual-Pathway Residual Network	It extracts features by cascading two dual-pathway residual networks [10].
DNN	Deep Neural Network	It is more accurate when is trained with augmented data [27].
DPU-Net	Dual Path U-Net	It has more convolutional layers and lower depth for each convolutional layer [29].
FCN	Fully Convolutional Network	It can multitask concurrently, and It can be used in complex segmentation tasks [14].
MMAN	Multimodality Aggregation Network	It provides good performance in brain segmentation [17].
RDAU-NET	Residual-Dilated-Attention-Gate-UNet	By increasing the layers, the network will have greater learning capacity [4].
RIANet	Recurrent Interleaved Attention Network	It has achieved competitive segmentation results with fewer parameters [30].
U-Net	Convolutional Networks for Biomedical Image Segmentation	It is a novel framework of CNN designed for precise and fast segmentation of images [13].
3D-SkipDenseSeg	3D Fully Convolutional, Skip-Connected DenseNet	It has highly accurate results particularly in applications with data-sparse [15].

3 Materials and Methods

3.1 Dataset Lung TIME

The computed tomography scans that were used correspond to the publicly available Lung TIME [24] dataset, which contains two subsets: TIME1 and TIME2. TIME1 includes 148 CT of adolescent patients and TIME2 contains 9 CT of adult patients from the Faculty Hospital in Motol, Prague, Czech Republic.

Each CT contains several images (slices) with a resolution of 512x512 pixels. In this work, 2003 slices were used and for each slice, binarization was performed for a constant threshold of -350 Hounsfield Units, proposed by Pulagam et al. [35] to separate the pulmonary region from CT. As preprocessing the images were rescaled in different resolutions: 32x32, 64x64 and 128x128 pixels. **Error! No se encuentra el origen de la referencia.** shows an example of a slice and its binarization in different

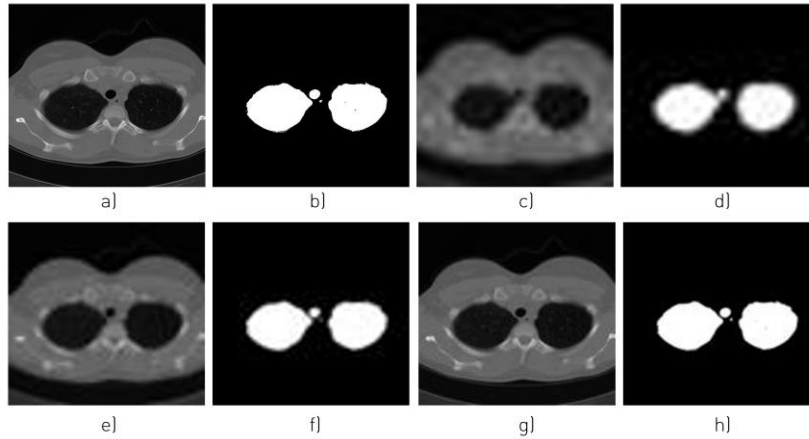


Fig. 1. Binarization and CT slice scaling a) original slice 512x512, b) binarized 512x512, c) slice 32x32, d) binarized 64x64, e) slice 64x64, f) slice 128x128, g) binarized 128x128.

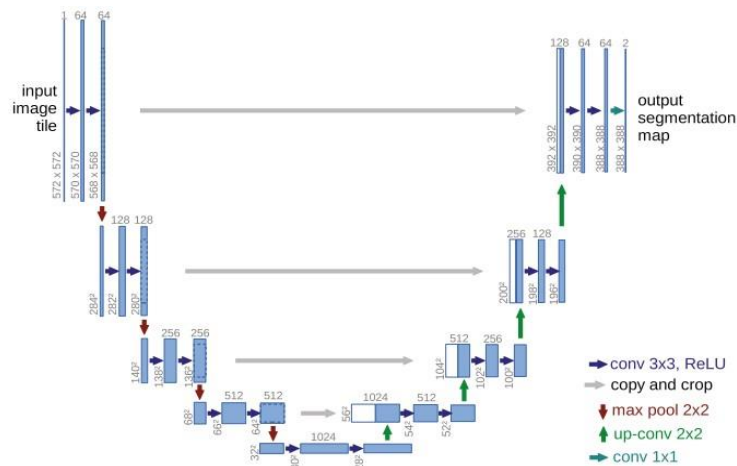


Fig. 2. The structure of U-Net [13].

resolutions of the image. Each of the 2003 slices and their respective binary image were used to train and evaluate the U-Net network.

3.2 U-Net

U-net is a convolutional neural network that allows to capture context and to achieve precise localization for precise and fast segmentation of images [13]. In this work, we applied U-Net using the Adam optimizer with a learning rate of 0.0001 and the binary cross-entropy loss function.

Table 2. Results of lung region segmentation using U-Net.

Input image	Epochs	Train ACC	Test ACC	Time (hours)
32x32	5	60.71%	60.14%	0.35
64x64	5	74.94%	74.28%	1.32
128x128	5	74.96%	74.26%	4.11
32x32	10	60.72%	60.65%	1.23
64x64	10	74.89%	74.84%	3.59
128x128	10	74.97%	74.50%	7.30

Table 3. Tools used in biomedical image segmentation.

Biomedical Image	Tools	Used in
CT	Python and Tensorflow	[9]
	PyTorch framework	[14]
MRI	Caffe framework	[15]
	Keras and Tensorflow	[16, 18]
	PyTorch framework	[14]
Ultrasound	MATLAB	[21]
	MATLAB and Dev C++	[34]
	Tensorflow	[22]
	Python using Keras and Tensorflow	[4,5]

Figure 2 shows the U-Net architecture. To implement U-Net, Tensorflow 2.0 and Python 3.7 were used. The laptop that was used has the following characteristics: Windows 10 operating system, Intel Core i3-5015U CPU @ 2.10 GHz (4 CPUs) and 6GB RAM.

Accuracy was calculated with different input image sizes (32x32, 64x64 and 128x128 pixels), using 70% of the slices for training and the remaining for testing.

4 Results and Discussion

Table 2 depicts the image input size, epochs number, the accuracy of the training and test, and the execution time for the training in hours by applying a U-Net architecture for the segmentation of the pulmonary region in Lung TIME dataset.

Table 4. Biomedical image segmentation using Neural Networks.

Technique	Image	Segmentation applied in	Results	Limitations/Challenges
CNN	MRI	Spinal cord and intra medullary lesions [16]	95% DICE in spinal cord	Is sensitive to the quality of the detection module.
			60% DICE in intramedullary multiple sclerosis	
	US	Prostate [22]	93.9 ± 3.5% DICE	12 hours of training.
		Breast [23]	85.1% JS	Is prone to errors in boundary of glandular tissues.
CNN & FCN	CT	Spine [9]	94% DICE, 97% SE, 99% SP	13 hours of training.
CDP-ResNet	CT	Lung nodules [10]	81.58% DICE	Is a semi-automatic segmentation method.
DNN	CT	Skeletal muscle at the L3 and T4 levels [11]	96.34 ± 2.77% JS	Their performance depends on the ground truth labels that are provided.
			98.11 ± 1.47% DICE 98.15 ± 1.63% SE, 99.81% SP	
DPU-Net	US	Arterial walls [29]	HD over 40 MHz dataset 87% JS in lumen and media HD over 20 MHz dataset 90% JS in lumen and media	A fixed-sized kernel cannot be a universal solution.
FCN	CT	Vertebra [14]	94.9 ± 2.1% DICE	Limitations in maximum number of filters per layer.
	MRI	Vertebral body [14]	94.4 ± 3.3% DICE	
MMAN	MRI	Brain [17]	DICE was 86.40% in GM, 89.70% in WM and 84.86% in CF	Its performance varies in different image modes.
RDAU-NET	US	Breast lesions [4]	DICE, SE and SP above 80%	Image resolution affects segmentation.
RIANet	MRI	Anatomical structures of the heart [30]	DICE 94.2% in left ventricular 92.3% in right ventricular and 91% in myocardium	Segmentation results of right ventricular is slightly worse.
U-Net	US	Breast [5]	DICE 82.5%	The detected contour can include a large area of non-tumor region, such as shadows.
3D- SkipDenseSeg	MRI	Brain [15]	DICE 90.37 ± 1.38% in WM, 92.27 ± 0.81% in GM and 95.79 ± 0.54% in CF	Sensitivity in computing the distances to the surfaces caused by the low contrast tissues between different classes.
U-Net	CT	Lung region	ACC above 60%	Image resolution affects segmentation accuracy and time of training.

It is observed that the accuracy (ACC) improves with increasing the input size of the slice and the number of epochs, however, the computational complexity increases.

Table 3 shows the tools used for biomedical image segmentation while table 4 shows a summary of the state-of-the-art techniques used in the segmentation of multimodal biomedical imaging specifically CT, MRI and ultrasound (US), using neural networks.

In addition, the limitations or challenges in each segmentation technique, have been presented. The different metrics that were used are Dice similarity coefficient (DICE), Jaccard Similarity (JS), Sensitivity (SE), Specificity (SP) and Accuracy (ACC). In the case of brain segmentation, the following symbology is used: Gray Matter (GM), White Matter (WM) and Cerebrospinal Fluid (CF).

Segmentation was applied in different human body structures such as spinal cord, spine, prostate, chest, lung, arteries and brain. As can be seen, variants of CNN networks [9, 14, 16] and deep learning [11] have performed better compared to other neural network architectures as CDP-ResNet [10] and MMAN [17].

However, CNN and deep learning require a lot of computing power in and the use of the same architecture does not generate the same accuracy in different types of biomedical images. Also, the areas of opportunity in segmentation of biomedical image using neural networks is to reduce computation time during testing and decrease errors in the partitioning of the boundary of tissues.

4 Conclusion

The segmentation of multimodal biomedical imaging is a great challenge and requires constant improvement in accuracy and performance, as it uses multiple images with noise, similar features and irregular shapes, which directly affects the tasks of classifying body structures and diseases prediction and prognosis. In addition, the increase in the dimensions of the images significantly increases the computational complexity of the algorithms.

As a result, various tools, methods and approaches are used in biomedical image segmentation. The metrics that the is generally used to evaluate segmentation performance is DICE score. Neural networks architectures have shown excellent results in the segmentation of multimodal biomedical imaging of CT, MRI and ultrasound.

There are many areas of improvement in neural networks, such as the reduction of training time, the search for kernel that can be used as universal solutions, the improvement of segmentation in the border tissues and the obtaining of results with less image training.

References

1. Toennies, K.: Guide to Medical Image Analysis. Springer (2017)
2. Dougherty, G.: Digital image processing for medical applications. Cambridge (2009)
3. Deserno, T.: Biomedical image processing. Springer (2011)
4. Zhuang, Z., Li, N., Joseph-Raj, A.N., Vijayalakshmi, G.V. Mahesh, Qiu, S.: An RDAU-NET model for lesion segmentation in breast ultrasound images. Plos One, 14(8) (2019)

5. Almajalid, R., Shan, J., Du, Y., Zhang, M.: Development of a deep-learning-based method for breast ultrasound image segmentation. In: 17th IEEE International Conference on Machine Learning and Applications (2018)
6. Bronzino, J.: Handbook of medical imaging. Academic Press (2000)
7. Koprowski, R.: Medical and biological image analysis. IntechOpen (2018)
8. González, D., Villuendas, Y., Argüelles, A.: Experimental comparison of bioinspired segmentation algorithms applied to segmentation of digital mammographies. *Research in Computing Science*, 138, pp. 109–116 (2017)
9. Vania, M., Mureja, D., Lee, D.: Automatic spine segmentation from CT images using convolutional neural network via redundant generation of class labels. *Journal of Computational Design and Engineering*, 6, pp. 224–232 (2019)
10. Liu, H., Cao, H., Song, E., Jin, R., Jin, Y., Hung, Ch.: A cascaded dual-pathway residual network for lung nodule segmentation in CT images. *Physica Medica*, 63, pp. 112–121 (2019)
11. Dabiri, S., Popuri, K., Cespedes-Feliciano, E.M., Caan, B.J., Baracos, V.E., Faisal-Beg, M.: Muscle segmentation in axial computed tomography (CT) images at the lumbar (L3) and thoracic (T4) levels for body composition analysis. *Computerized Medical Imaging and Graphics*, 75, pp. 47–55 (2019)
12. Long, J., Shelhamer, E., Darrell, T.: Fully convolutional networks for semantic segmentation. In: The IEEE Conference on Computer Vision and Pattern Recognition, pp. 3431–3440 (2015)
13. Ronneberger, O., Fischer, P., Brox, T.: U-Net: convolutional networks for biomedical image segmentation. In: *Medical Image Computing and Computer-Assisted Intervention*, pp. 234–241 (2015)
14. Lessmann, N., van Ginneken, B., de Jong, P.A., Išguma, I.: Iterative fully convolutional neural networks for automatic vertebra segmentation and identification. *Medical Image Analysis*, 53, pp. 142–155 (2019)
15. Bui, T., Shin, J., Moon, T.: Skip-connected 3D DenseNet for volumetric infant brain MRI segmentation. *Physica Medica*, 54 (2019)
16. Gros, C., De Leener, B., Badji, A., Maranzano, J., Eden, D., Dupont, S.M., Talbot, J., Zhuoquiong, R., Liu, Y., Granberg, T., Ouellette, R., et al.: Automatic segmentation of the spinal cord and intramedullary multiplesclerosis lesions with convolutional neural networks. *Neuroimage*, 184, pp. 901–915 (2019)
17. Li, J., Yu, Z.L., Gu, Z., Liu, H., Li, Y.: MMAN: Multi-modality aggregation network for brain segmentation from MR images. *Neurocomputing*, 358, pp. 10–19 (2019)
18. Rak, M., Steffen, J., Meyer, A., Hansen, C., Tönnies, K.D.: Combining convolutional neural networks and star convex cuts for fast whole spine vertebra segmentation in MRI. *Computer Methods and Programs in Biomedicine*, 177, pp. 47–56 (2019)
19. Rak, M., Tönnies, K.: A learning-free approach to whole spine vertebra localization in MRI. In: *Medical Image Computing and Computer-Assisted Intervention*, pp. 283–290 (2016)
20. Ilhan, U., Ilhan, A.: Brain tumor segmentation based on a new threshold approach. *Procedia Computer Science*, 120, pp. 580–587 (2018)
21. Nithya, A., Appathurai, A., Venkatadri, N., Ramji, D.R., Anna-Palagand, C.: Kidney disease detection and segmentation using artificial neural network and multi-kernel k-means clustering for ultrasound images. *Measurement*, 149 (2019)
22. Karimi, D., Zeng, Q., Mathur, P., Avinash, A., Mahdavi, S., Spadinger, I., Abolmaesumi, P., Salcudean, S.E.: Accurate and robust deep learning-based segmentation of the prostate clinical target volume in ultrasound images. *Medical Image Analysis*, 57, pp. 186–195 (2019)

23. Xu, Y., Wang, Y., Yuan, J., Cheng, Q., Wang, X., Carson, P.L.: Medical breast ultrasound image segmentation by machine learning. *Ultrasonics*, 91, pp. 1–9 (2019)
24. Dolejší, M., Kybic, J.: The lung time—annotated lung nodule dataset and nodule detection framework. In: *Proceedings of SPIE*, 7260 (2009)
25. van Sloun, R.J.G., Wildeboer, R.R., Mannaerts, C.K., Postema, A.W., Gayet, M., Harrie, Beerlage, H.P., Salomon, G., Wijkstra, H., Mischi, M.: Deep learning for real-time, automatic, and scanner-adapted prostate (zone) segmentation of transrectal ultrasound, for example, magnetic resonance imaging–transrectal ultrasound fusion prostate biopsy. *European Urology Focus* (2019)
26. Simard, P., Steinkraus, D., Platt, J.: Best practices for convolutional neural networks applied to visual document analysis. In: *Seventh International Conference on Document Analysis and Recognition* (2003)
27. Liu, C., Gardner, S., Wen, N., Elshaikh, M.A., Siddiqui, F., Movsas, B., Chetty, I.J.: Automatic segmentation of the prostate on CT images using deep neural networks (DNN). *International Journal of Radiation Oncology Biology Physics*, 104(4), pp. 924–932 (2019)
28. Huang, X., Sun, W., Tseng, T.L., Li, Ch., Qian, W.: Fast and fully-automated detection and segmentation of pulmonary nodules in thoracic ct scans using deep convolutional neural networks. *Computerized Medical Imaging and Graphics*, 74, pp. 25–36 (2019)
29. Yang, J., Faraji, M., Basu, A.: Robust segmentation of arterial walls in intravascular ultrasound images using dual path U-Net. *Ultrasonics*, 96, pp. 24–33 (2019)
30. Tong, Q., Li, C., Si, W., Liao, X., Tong, Y., Yuan, Z., Heng, P.A.: RIANet: Recurrent interleaved attention network for cardiac MRI segmentation. *Computers in Biology and Medicine* (2019)
31. Lu, G., Zhou, L.: Localization of prostatic tumor’s infection based on normalized mutual information MRI image segmentation. *Journal of Infection and Public Health* (2019)
32. Sheela, A., Suganthi, G.: Automatic brain tumor segmentation from MRI using greedy snake model and fuzzy C-Means optimization. *Journal of King Saud University - Computer and Information Sciences* (2019)
33. Yang, T., Song, J., Li, L.: A deep learning model integrating SK-TPCNN and random forests for brain tumor segmentation in MRI. *Biocybernetics and Biomedical Engineering*, 39, pp. 613–623 (2019)
34. Panigrahi, L., Verma, K., Singh, B.K.: Ultrasound image segmentation using a novel multi-scale gaussian kernel fuzzy clustering and multi-scale vector field convolution. *Expert Systems with Applications*, 115, pp. 486–498 (2019)
35. Pulagam, A., Rao, V., Inampudi, R.: Automated pulmonary lung nodule detection using an optimal manifold statistical based feature descriptor and SVM classifier. *Biomedical and Pharmacology Journal*, 10(3), pp. 1311–1324 (2017)